JACS
JOURNAL OF THE AMERICAN CHEMICAL SOCIETY
pubs.acs.org/JACS
Article

Sugar-Fueled Dissipative Living Materials

Hyuna Jo, Serxho Selmani, Zhibin Guan, and Seunghyun Sim*

Cite This: J. Am. Chem. Soc. 2023, 145, 1811−1817
Read Online
ACCESS | Metrics & More | Article Recommendations | Supporting Information

ABSTRACT: Dissipative behaviors in biology are fuel-driven processes controlled by living cells, and they shape the structural and functional complexities in biological materials. This concept has inspired the development of various forms of synthetic dissipative materials controlled by time-dependent consumption of chemical or physical fuels, such as reactive chemical species, light, and electricity. To date, synthetic living materials featuring dissipative behaviors directly controlled by the fuel consumption of their constituent cells is unprecedented. In this paper, we report a chemical fuel-driven dissipative behavior of living materials comprising *Staphylococcus epidermidis* and telechelic block copolymers. The macroscopic phase transition is controlled by D-glucose which serves a dual role of a competitive disassembling agent and a biological fuel source for living cells. Our work is a significant step toward constructing a synthetic dissipative living system and provides a new tool and knowledge to design emergent living materials.

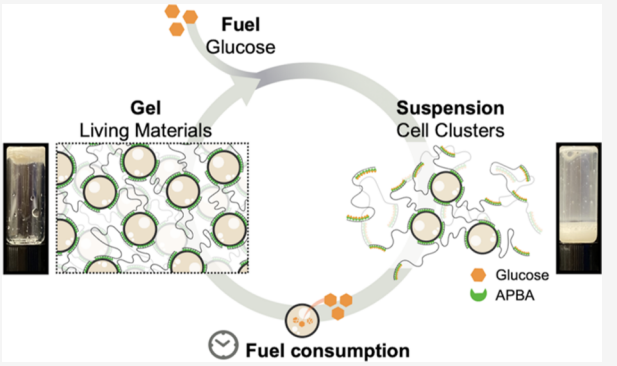

INTRODUCTION

Dissipative behaviors sculpt the structural and functional complexities of living biological materials.[1,2] The out-of-equilibrium nature of these biological processes accompanies the flow of energy and consumption of fuel sources by living cells. For example, bone tissues—a composite living material of cells and macromolecular scaffold—undergo continuous remodeling to repair damages, adjust for changing mechanical needs, and maintain calcium homeostasis.[3−5] In this and many other examples in biological materials, the cellular metabolism of fuels (e.g., glucose) is the fundamental driving force controlling their macroscopic behaviors.

Efforts in the past decade to mimic such out-of-equilibrium control in constructing molecular assemblies have yielded various forms of synthetic dissipative materials. Pioneering works in this area have demonstrated molecular assemblies driven by chemical reaction networks where the added fuel converts a precursor into an assembling or a disassembling species and a spontaneous chemical process (e.g., hydrolysis) reverts it to the precursor state.[6−9] In these systems, the chemical energy in the fuel temporarily produces a transient metastable species, while the fuel is converted into waste.[10−13] Other forms of energy to generate metastable states, including light,[14−16] and more recently, electricity,[17] have been introduced to construct and control dissipative materials.

An important challenge in this field is to integrate such dissipative behaviors in synthetic materials with living cells to create synthetic living materials equipped with time-dependent behaviors useful for shaping their structure and function, just like what is seen in bones. An effort to indirectly connect the dissipative behavior of synthetic materials with cellular metabolism was made by Miravet and Angulo-Pachón.[18] They showed that CO_2 produced by the metabolism of sucrose by yeast cells changes the pH of the solution, inducing subsequent assembly of hydrogelators. However, synthetic living material featuring time-dependent dissipative behavior directly controlled by the cellular metabolism of fuel is unprecedented.

Here, we report a chemical fuel-driven dissipative living material comprising bacterial cells and a telechelic block polymer containing 3-acetamidophenylboronic acid (APBA) end blocks (Figure 1). In a previous study, we reported a series of living materials enabled by dynamic covalent bond formation between the diols on the surface teichoic acids of *Bacillus subtilis* and the phenylboronic acid moiety on synthetic block copolymers.[19] These living materials disassemble upon addition of competing diols such as fructose. Given that sugars can be consumed as a fuel source for living cells, we sought to capitalize on the dual role of D-glucose, as a competitive disassembling agent and a biological fuel source for cells, to create the first dissipative living material system.

Received: October 19, 2022
Published: January 9, 2023

https://doi.org/10.1021/jacs.2c11122
J. Am. Chem. Soc. 2023, 145, 1811−1817

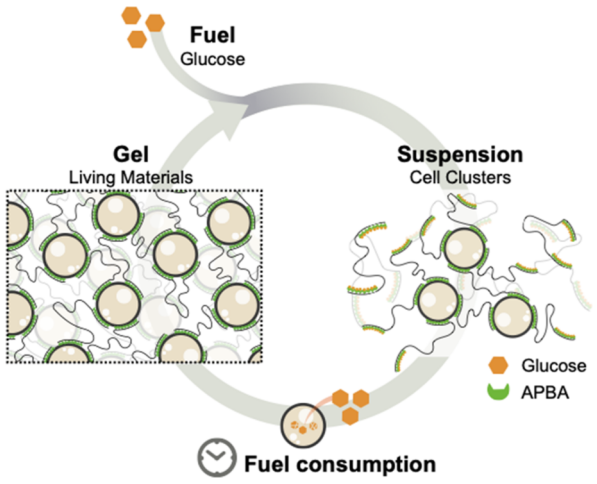

Figure 1. Design concept of fuel-driven dissipative living materials. A living material (gel) comprising *Staphylococcus epidermidis* and a telechelic block copolymer bearing an APBA end block disassemble into cell clusters (suspension) following the addition of D-glucose (fuel). Time-dependent metabolic fuel consumption by living cells drives the reassembly of living materials.

RESULTS AND DISCUSSION

Interplay between Competitive Binding to Polymers and Metabolic Consumption of Fuels Leads to Dissipative Behaviors in Cellular Aggregates. The bacterium in our previous study, *B. subtilis*, undergoes sporulation in nutrient-deprived conditions. Because this process hinders continuous metabolic consumption of fuels and releases cellular debris as byproducts, we chose a non-sporulating Gram-positive bacterium, *S. epidermidis*, for this study. Its thick peptidoglycan wall is decorated with teichoic acids and enables survival under various osmotic pressures.[20] We first set out to examine whether the APBA motif can target the available surface diols on *S. epidermidis*. Fluorescent probes appended with a sulfo-Cy5 (sCy5) dye [Figure 2a, 7.5 μM in phosphate-buffered saline (PBS), pH 7.2] were incubated with suspensions of *S. epidermidis* for 3 h at room temperature, washed with PBS twice, and subjected to fluorescence microscopy (λ_{ex} = 630 nm; λ_{obs} = 690−740 nm).[19] Fluorescence signals from the monomeric APBA probe, APBA-sCy5, were localized on the cell surface, and individual cells were mostly dispersed (Figure 2b). In contrast, fluorescent cellular aggregates were observed with the polymeric probe (Figure 2c), poly(APBA)-sCy5, suggesting that these polymers can provide binding sites for more than one cell. Corresponding to these observations, the bulk fluorescence emission (λ_{ex} = 630 nm; λ_{obs} = 650−800 nm) of these samples revealed that APBA-containing probes showed much stronger fluorescence than the cell suspension treated with the Tris-sCy5 probe that bears a trisaminomethane group instead of the APBA motif (Figure 2d). These results support that the APBA motif binds to the *S. epidermidis* cell surface, similar to *B. subtilis*.[19]

Next, we proceeded with our design of dissipative living materials by assuming that metabolizable diols, such as fructose and glucose, can serve dual roles in this system: (1) as a competitive detaching agent to separate cells from polymers and (2) as a carbon source spontaneously metabolized by living cells over time. Three sugars were used in this study: D-glucose, L-glucose, and D-fructose. All of these sugars are known to bind to the APBA motif with different association coefficients,[21] 8.1 M^{-1}

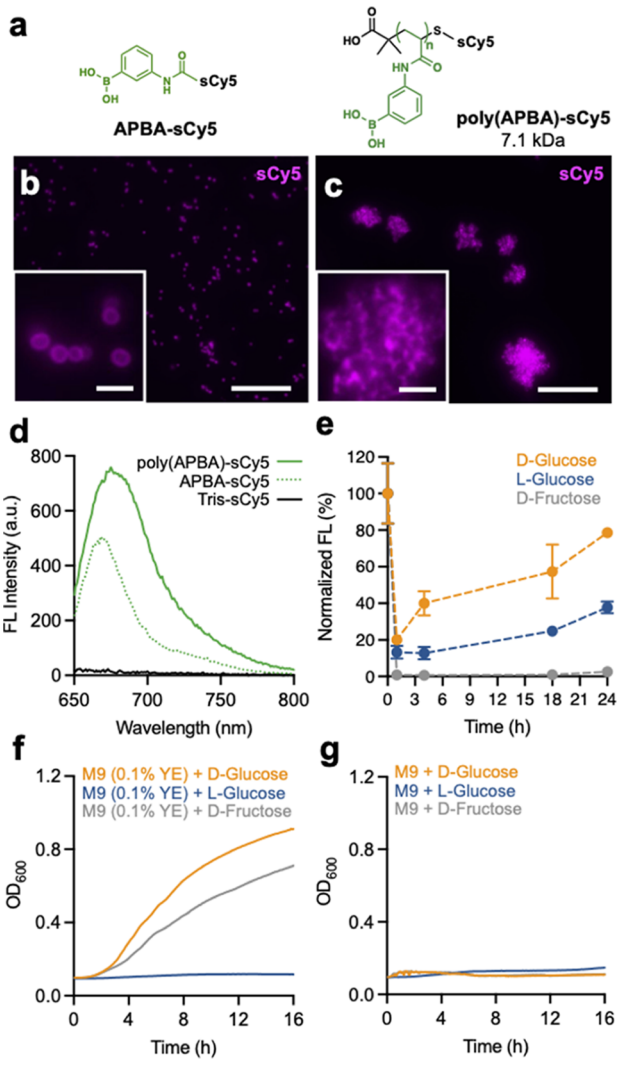

Figure 2. Interplay between competitive binding to polymers and metabolic consumption of fuels leads to dissipative behaviors in cellular aggregates. (a) Molecular structure of monomeric and polymeric APBA probes bearing a sulfo-Cy5 dye. (b,c) Representative fluorescence microscopy images (λ_{ex} = 630 nm; λ_{obs} = 690−740 nm) of *S. epidermidis* cells incubated with (b) APBA-sCy5 and (c) poly(APBA)-sCy5. Scale bars = 30 μm (3 μm for inset). (d) Bulk fluorescence emission spectra (λ_{ex} = 630 nm) of *S. epidermidis* cells after 3 h of incubation with APBA-sCy5 (green, solid line), polyAPBA-sCy5 (green, dotted line), and Tris-sCy5 (black). (e) Normalized fluorescence profiles of *S. epidermidis* cell suspension first incubated with poly(APBA)-sCy5 and subsequently treated with D-glucose (orange), L-glucose (blue), and D-fructose (gray) over 24 h. N = 3 (biological replicates). Error bars represent ±s.e.m. (f,g) Cell density probed by absorbance at 600 nm (OD_{600}) of M9 media containing D-glucose (orange), L-glucose (blue), and D-fructose (gray) in the presence (f) and in the absence (g) of 0.1% yeast extract.

for glucose and 350 M^{-1} for fructose. We tested the dynamic behavior of bound APBA probes in the presence of these sugars by adding them (500 mM) to suspensions of labeled cells with poly(APBA)-sCy5 in PBS. At each time point, cells were washed to remove any unbound fluorescent species, and the remaining fluorescence emission from bound polymers was measured. Just after 1 h of incubation, we observed approximately 80% decrease in fluorescence intensity in samples incubated with D- and L-glucose and near complete diminishment of fluorescent signals with D-fructose (Figure 2e). This agrees with the fact that

https://doi.org/10.1021/jacs.2c11122
J. Am. Chem. Soc. 2023, 145, 1811−1817

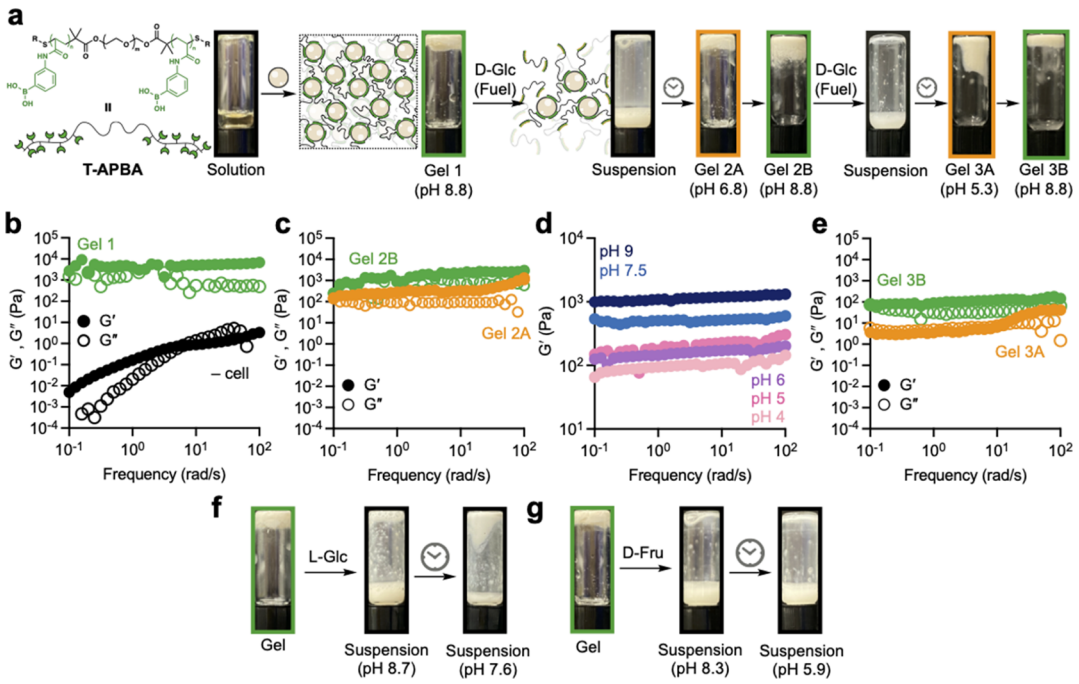

Figure 3. Glucose-driven dissipative behavior of living materials. (a) Schematic illustration and optical images of living materials showing dissipative behaviors. Gel 1, comprising T-APBA and *S. epidermidis*, disassembles into cell suspension by exogenously supplied D-glucose (fuel) and turns back into Gel 2A. After adjusting the pH, Gel 2B is subjected to another cycle, yielding a cell suspension, followed by Gel 3A and 3B. (b) Storage moduli G' and loss moduli G'' of T-APBA in the absence (black) and in the presence (green) of *S. epidermidis*. (c) Rheological characterization of Gel 2A and Gel 2B. (d) G' values of living materials incubated at pH 4–9 for 18 h at 30 °C. (e) Rheological characterization of Gel 3A and Gel 3B. (f,g) Optical images of living materials after immersing them into an (f) L-glucose or (g) D-fructose solution.

fructose binding to APBA is 2 orders of magnitude stronger than glucose.[21] Microscopic observation of cells at this time point shows that large fluorescent cellular aggregates disperse into individual cells with diminished fluorescence on their surface for all of the sugars (Figure S4). With prolonged incubation time, the fluorescence from bound polymers increases in the samples containing D-glucose (Figure 2e, orange), suggesting that consumption of this sugar by cellular metabolism frees APBA binding sites from polymers and leads to reattachment to the cell surface. We also observed an increment of fluorescence in the samples incubated with L-glucose after 18 h (Figure 2e, navy blue). In contrast, diminished fluorescence in the samples incubated with D-fructose did not recover (Figure 2e, gray). Corresponding to the bulk fluorescence measurements, fluorescent cellular aggregates were observed in cells incubated with D- and L-glucose for 24 h (Figure S4).

To investigate whether *S. epidermidis* cells metabolize these sugars, we first prepared M9 media supplemented with 0.1% yeast extract containing nitrogen and other necessary elements for cell division. Because cells in this media do not divide without providing extra carbon sources (Figure S7), it allows us to test whether *S. epidermidis* can metabolize these sugars by monitoring the cell density (OD_{600}) over time. In the presence of D-glucose and D-fructose (500 mM, 30 °C), *S. epidermidis* cells actively divide in the course of 16 h (Figure 2f). However, this is not the case in the medium supplemented with L-glucose. This result demonstrates that *S. epidermidis* utilizes D-glucose and D-fructose as carbon sources but not L-glucose. It also supports our conclusion that cellular consumption of D-glucose over time leads to the reattachment of polymers to the cell surface (Figure 2e, orange). Despite the fact that D-fructose is consumed by *S. epidermidis*, detached polymers did not reattach to the cell surface even after 24 h (Figure 2e, gray). We suspect that because fructose binds too strongly to the polymers, they are less available for cells to consume. To understand the small, yet noticeable increase in fluorescence in samples treated with L-glucose (Figure 2e, navy blue), we measured the pH of these solutions over the course of 24 h and performed the Alizarin red S (ARS) dye displacement assay with APBA-containing polymer at different pHs.[22] We observed a significant drop in pH in all three sugar solutions due to cellular metabolic activities (Figure S16). On the other hand, the fluorescence decay from the diol exchange reaction at APBA sites is more prominent at higher pHs (Figure S17). Based on these results, we suspect that the decreased pH due to the respiratory activity of the cells lowers the binding affinity of L-glucose to APBA-containing polymers, resulting in the formation of cell aggregates at later time points. Experiments performed in M9 media without 0.1% yeast extract show that cell division does not occur even when carbon sources are present (Figure 2g). All of the living materials described below are prepared without yeast extract to suppress cell division.

Fuel-Driven Dissipative Behavior of Living Materials. Encouraged by the results shown above, we synthesized a telechelic polymer, T-APBA [Figure 3a; 16 740 g/mol, poly(ethylene glycol) (PEG) 10 000 g/mol as the mid-block, and 44 units of APBA as the end-block],[19] to construct macroscopic living materials showing dissipative behavior. A PBS suspension of *S. epidermidis* cells (10^{11} cells/mL in PBS, pH 7.2) was added to a solution of T-APBA (10 wt % in 80 mM PBS, pH 9.5) to afford a living material in the hydrogel form (Gel 1) (Figure 3a). Linear rheological measurement showed that adding cells to a polymer solution (Figure 3b, black) makes it a viscoelastic solid (Figure 3b, green). Immersing and agitating Gel 1 in a D-glucose solution (500 mM in M9, pH 8.1, 200 rpm, Figure S8) at 30 °C for 3 h converts the macroscopic network into a suspension of

https://doi.org/10.1021/jacs.2c11122
J. Am. Chem. Soc. 2023, 145, 1811–1817

cell clusters (Figures 3a and S8). Further incubation and agitation of this suspension at 30 °C for 14 more hours resulted in the reformation of a macroscopic gel (Gel 2A, Figure 3a), a viscoelastic solid with shear storage moduli (G') an order of magnitude lower than that of pristine Gel 1 (Figure 3c, orange). Notably, the pH of this Gel 2A (pH 6.8) was significantly lower than the pristine Gel 1 (pH 8.8) and the glucose solution (pH 8.1), presumably due to the active cellular metabolism and consumption of carbon sources producing organic acids, such as pyruvic acid or acetic acid (Figure S16).[23]

We suspect that the lower G' in Gel 2A is due to the lowered pH (pH 6.8) because the diol binding of phenylboronic acid species is known to be affected by pH.[21,24,25] To establish the pH-dependent changes in G', we prepared Gel 1 samples and immersed them in PBS buffers with a pH ranging from 4 to 9. As the pH increases, G' of Gel 1 also increases (Figure 3d). Based on this result, we adjusted the pH of Gel 2A from 6.8 to 8.8 (Gel 2B), after which G' of Gel 2B increased by an order of magnitude (Figure 3c, green). Immersing Gel 2B to the glucose solution (500 mM in M9, pH 8.1, 200 rpm) for the second time yielded a suspension (Figure S8), and further incubation of this suspension regenerates the macroscopic network, Gel 3A (Figure 3e, orange). We note that if the pH of Gel 2A is not adjusted before subjecting them to the second cycle, it fails to generate Gel 3A. Similar to Gel 2A, Gel 3A was more acidic (pH 5.3) and exhibited lower G' compared to Gel 2B due to the metabolic production of acidic species. Even after adjusting its pH to 8.8 (Gel 3B), G' of the gel was significantly lower than the pristine (Gel 1) or reformed gels after the first cycle (Gel 2A and 2B) (Figure 3e, green). Using a 5-cyano-2,3-ditolyl tetrazolium chloride reagent, we investigated the metabolic activity of the retrieved cells from these gels. By the end of the second cycle, the cellular metabolic activity is decreased by 50% (Figure S12). We suspect that the reduced metabolic consumption of glucose and released cellular debris (e.g., nucleic acids) from dead cells weakened the mechanical stiffness of Gel 3A and 3B.

When Gel 1 is exposed to a solution of L-glucose (500 mM in M9, pH 8.1), the suspension does not form a gel even after 17 h (Figures 3f and S9). The complex viscosity of the L-glucose suspension increased by 8.3-fold during this time (Figure S9), and the pH of this suspension decreased from 8.7 to 7.6. We speculate that cellular respiration lowered the pH of the suspension and changed the relative binding affinity of added L-glucose and the APBA motif (Figures S16 and S17). When Gel 1 is immersed in a D-fructose solution (500 mM in M9, pH 8.1), the suspension also did not revert to the gel form (Figure 3g), and the complex viscosity of the suspension after 17 h of incubation did not increase from that of 3 h (Figure S10). The pH of this suspension also decreased from 8.3 to 5.9, presumably due to the cellular respiration and partial consumption of D-fructose. These trends are similar to the fluorescence data obtained with cellular aggregates formed by added poly(APBA) (Figure 2e).

Effect of Polymer Structures on Dissipative Behavior. We then investigated whether polymer structures affect the dissipative behavior of the resulting living materials. A statistical copolymer with APBA motifs distributed along the polymer chain (S-APBA; Figure 4a) was synthesized via reversible addition−fragmentation chain transfer polymerization and subsequent end-group modification (Figures S1 and S2). This polymer lacks the PEG domain and instead has *N*-hydroxyethyl acrylamide comonomers. S-APBA (17 413 g/mol) has a similar molecular weight to T-APBA (16 740 g/mol), according to gel permeation chromatography (Figure S3), and contains a similar number of APBA units per polymer chain (40 for S-APBA and 44 for T-APBA), based on ^{1}H NMR (Figures S1 and S2). We prepared a self-standing hydrogel by adding a cell suspension (10^{11} cells/mL) to a solution of S-APBA (20 wt % in methanol) (Figure 4b). Similar to the case of T-APBA, adding cells to the polymer solution increased the G' by orders of magnitude (Figure 4c). These living materials were converted into suspension by immersing and agitating them in a D-glucose solution (500 mM in M9, pH 8.1) and, strikingly, it did not reform the macroscopic network even after 17 h of incubation (Figures 4b and S11). The fact that S-APBA is incapable of generating dissipative behavior in living materials implies the potential multivalent effect of APBA end blocks of telechelic polymers in cellular binding.

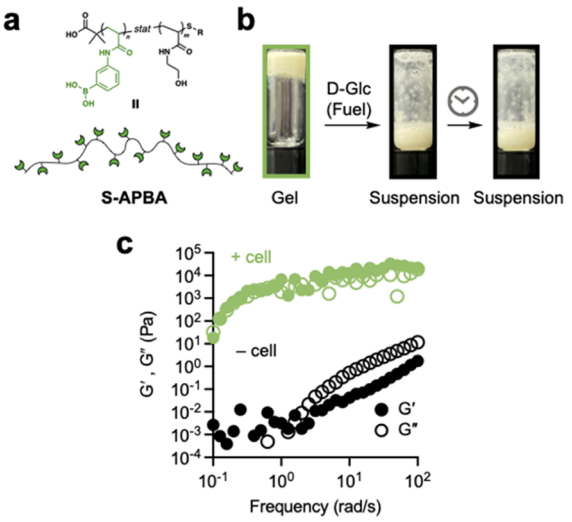

Figure 4. Effect of polymer structures on dissipative behavior. (a) Molecular structure of a statistical copolymer S-APBA bearing *N*-hydroxyethyl acrylamide and APBA. (b) Optical images of living materials comprising S-APBA and *S. epidermidis* after immersing them in a D-glucose solution. (c) Storage moduli G' and loss moduli G'' of S-APBA in the absence (black) and in the presence (green) of *S. epidermidis*.

Time-Dependent Fuel Consumption by Living Cells. Finally, we investigated D-glucose consumption by living materials at a molecular level. We quantified the extracellular concentration of glucose in living materials under dissipative cycles using colorimetric assays (Figure S14). The concentration of D-glucose was reduced by 92% in 17 h in the course of the first cycle (Figure 5a). In contrast, the amount of D-glucose was decreased by only 58% during the second cycle, which corresponds to the weak mechanical properties of Gel 3A and 3B (Figure 2e) and reduced metabolic activity of encased cells (Figure S12). We employed a fluorescently labeled D-glucose probe to further investigate whether glucose was transported intracellularly to be consumed.[26] The cells treated with this probe were retrieved from the living materials for bulk fluorescence measurements (Figure 5b) and fluorescence microscopy (Figures 5c and S5). Both results show more intracellularly localized fluorescent probes as time goes by. Similar to glucose, intracellular localization of fluorescently labeled fructose was observed (Figure S6). In addition, LC−MS/MS analyses revealed the consumption of D-glucose and D-fructose over time but not L-glucose (Figure S15). Taken together, the dissipative behavior of living materials is directly

https://doi.org/10.1021/jacs.2c11122
J. Am. Chem. Soc. 2023, 145, 1811−1817

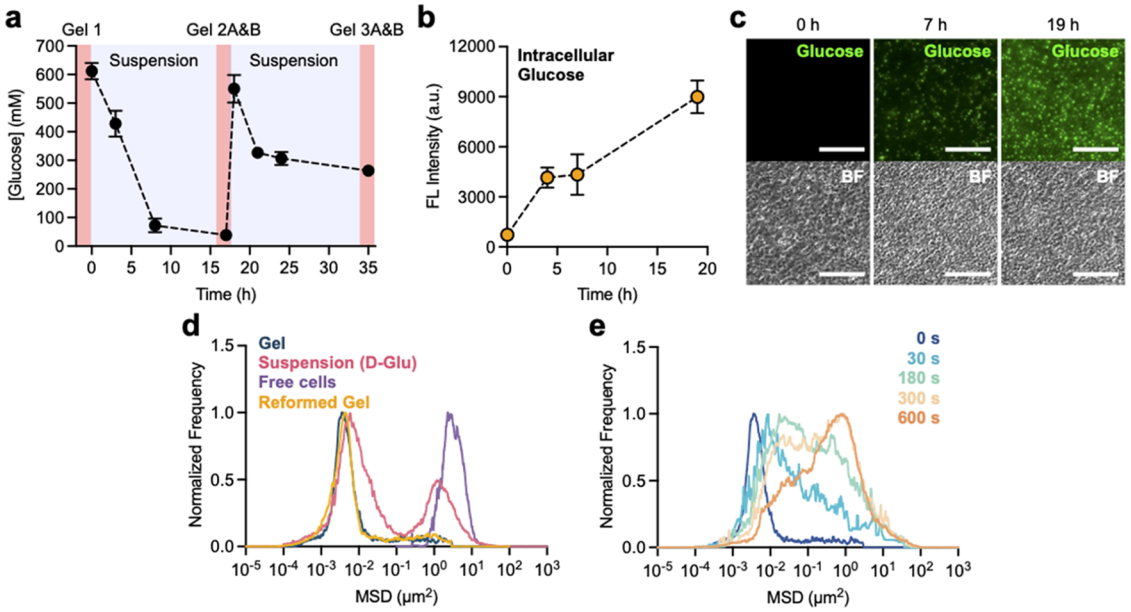

Figure 5. Time-dependent fuel consumption and cell mobility. (a) Extracellular concentration of supplied D-glucose over time. (b) Fluorescence emission of bulk suspensions of cells retrieved from living materials (λ_{ex} = 480 nm; λ_{obs} = 520 nm) and (c) fluorescence microscopy images (λ_{ex} = 480 nm; λ_{obs} = 520 nm) of the retrieved cells from living materials. These materials were incubated with a solution containing the fluorescently-labeled glucose probe. Scale bars = 20 μm. (d) MSD profile of cells in pristine gel, cell suspension prepared with D-glucose, free-floating cells, and cells in reformed gel. (e) MSD profiles of cells after in situ addition of D-glucose to a pristine gel.

driven by the time-dependent consumption of supplied glucose via cellular metabolism.

Because cells are the crosslinking points of these living materials, their mobility should correlate with the macroscopic behavior of materials and give us molecular insights into the fuel consumption process. We observed fluorescently labeled cells within living materials and cell clusters to examine cellular mobility using confocal laser scanning microscopy (CLSM). About 1% of the cells within the living materials were covalently labeled with NHS-sCy5 to allow for individual cell tracking to compute each sample's mean-square displacement (MSD) profile for the cell movement (Videos S1, S2, S3, S4, Figure S18). As shown in Figure 5d, gels, suspensions, and free-floating cell samples showed distinct MSD profiles. Cells embedded in the living materials showed much slower movement compared to free-floating cells by a factor of ~10^3. The suspension prepared by soaking living materials in D-glucose solution shows two distinct populations, one close to free-floating cells and the other resembling cells embedded in the gel, indicating the coexistence of single cells and cell clusters. Notably, reformed gels showed a similar MSD profile to pristine gels. We then monitored the in situ dissociation of living materials upon addition of D-glucose to the sample. Dissociation of cells from the edge of the gel was monitored by CLSM over time (Figures 5e, S18, and Video S5). The population shifted to mostly free-floating cells in the course of 600 s in response to the added D-glucose.

CONCLUSIONS AND OUTLOOK

This work reports the first dissipative living material controlled by metabolization of D-glucose by living cells. Because these materials are constructed with the dynamic covalent interface between living cells and telechelic block copolymers, D-glucose can serve as both a disassembling agent and a metabolic fuel for the living materials. As a result, the macroscopic phase transition was directly controlled by the fuel consumption of living cells over time. We also investigated the effect of polymer architecture, sugar structure, and kinetics of fuel consumption at a molecular level. To the best of our knowledge, this work represents the first example of a synthetic dissipative system that directly interfaces with and is controlled by living cells. It significantly expands the scope of dissipative materials by bringing it one step closer to biology. Considering that biology harnesses time-dependent restructuring mechanisms to shape many functions, this and further work may open up new possibilities for creating complex living materials with emergent functions.

ASSOCIATED CONTENT

Supporting Information

The Supporting Information is available free of charge at https://pubs.acs.org/doi/10.1021/jacs.2c11122.

Materials, instrumentation, experimental and synthetic methods, ^{1}H NMR spectra, gel permeation chromatography measurement, fluorescence microscopy results, growth curves, rheological characterization, cell viability tests, sugar assays, pH measurements, ARS assays, and XY trajectories of fluorescently labeled cells (PDF)

Visualization of free-floating cells, as shown in Figure 5d (MOV)

Visualization of cells within pristine gels, as shown in Figure 5d (MOV)

Visualization of cells in suspensions, as shown in Figure 5d (MOV)

Visualization of cells within reformed gels, as shown in Figure 5d (MOV)

Visualization of in situ disassociation of gel, as shown in Figure 5e (MOV)

https://doi.org/10.1021/jacs.2c11122
J. Am. Chem. Soc. 2023, 145, 1811−1817

AUTHOR INFORMATION

Corresponding Author

Seunghyun Sim − *Center for Complex and Active Materials, University of California, Irvine, Irvine, California 92697, United States; Department of Chemistry, University of California Irvine, Irvine, California 92697, United States; Department of Chemical and Biomolecular Engineering and Department of Biomedical Engineering, University of California Irvine, Irvine, California 92697, United States;* orcid.org/0000-0002-4232-5917; Email: s.sim@uci.edu

Authors

Hyuna Jo − *Center for Complex and Active Materials, University of California, Irvine, Irvine, California 92697, United States; Department of Chemistry, University of California Irvine, Irvine, California 92697, United States*

Serxho Selmani − *Center for Complex and Active Materials, University of California, Irvine, Irvine, California 92697, United States; Department of Chemistry, University of California Irvine, Irvine, California 92697, United States*

Zhibin Guan − *Center for Complex and Active Materials, University of California, Irvine, Irvine, California 92697, United States; Department of Chemistry, University of California Irvine, Irvine, California 92697, United States; Department of Chemical and Biomolecular Engineering, Department of Material Science and Engineering, and Department of Biomedical Engineering, University of California Irvine, Irvine, California 92697, United States;* orcid.org/0000-0003-1370-1511

Complete contact information is available at: https://pubs.acs.org/10.1021/jacs.2c11122

Author Contributions

The manuscript was written through contributions of all authors, and all authors have given approval to the final version of the manuscript.

Notes

The authors declare no competing financial interest.

ACKNOWLEDGMENTS

This work was primarily supported by the National Science Foundation Materials Research Science and Engineering Center program through the UC Irvine Center for Complex and Active Materials (DMR-2011967). The work was partially supported by the US Department of Energy, Office of Science, Basic Energy Sciences (DE-FG02-04ER46162, Z.G.) and the National Science Foundation (CHE-1904939, Z.G.). The authors acknowledge the use of facilities and instrumentation at the UC Irvine Materials Research Institute (IMRI) supported in part by the National Science Foundation Materials Research Science and Engineering Center program through the UC Irvine Center for Complex and Active Materials (DMR-2011967). S.S. acknowledges support from an NSERC postdoctoral fellowship from the Research Council of Canada. Nuclear Magnetic Resonance measurements were done in the NMR facility in the Department of Chemistry, University of California, Irvine.

REFERENCES

(1) Karsenti, E. Self-organization in cell biology: a brief history. *Nat. Rev. Mol. Cell Biol.* **2008**, *9*, 255−262.

(2) Lenne, P.-F.; Trivedi, V. Sculpting tissues by phase transitions. *Nat. Commun.* **2022**, *13*, 664.

(3) Lee, W.-C.; Guntur, A. R.; Long, F.; Rosen, C. J. Energy metabolism of the osteoblast: implications for osteoporosis. *Endocr. Rev.* **2017**, *38*, 255−266.

(4) Hadjidakis, D. J.; Androulakis, I. I. Bone remodeling. *Ann. N. Y. Acad. Sci.* **2006**, *1092*, 385−396.

(5) Raggatt, L. J.; Partridge, N. C. Cellular and molecular mechanisms of bone remodeling. *J. Biol. Chem.* **2010**, *285*, 25103−25108.

(6) Boekhoven, J.; Brizard, A. M.; Kowlgi, K. N.; Koper, G. J.; Eelkema, R.; van Esch, J. H. Dissipative Self-Assembly of a Molecular Gelator by Using a Chemical Fuel. *Angew. Chem.* **2010**, *122*, 4935−4938.

(7) Boekhoven, J.; Hendriksen, W. E.; Koper, G. J.; Eelkema, R.; van Esch, J. H. Transient assembly of active materials fueled by a chemical reaction. *Science* **2015**, *349*, 1075−1079.

(8) Maiti, S.; Fortunati, I.; Ferrante, C.; Scrimin, P.; Prins, L. J. Dissipative self-assembly of vesicular nanoreactors. *Nat. Chem.* **2016**, *8*, 725−731.

(9) Leira-Iglesias, J.; Sorrenti, A.; Sato, A.; Dunne, P. A.; Hermans, T. M. Supramolecular pathway selection of perylenediimides mediated by chemical fuels. *Chem. Commun.* **2016**, *52*, 9009−9012.

(10) Sharko, A.; Livitz, D.; De Piccoli, S.; Bishop, K. J.; Hermans, T. M. Insights into Chemically Fueled Supramolecular Polymers. *Chem. Rev.* **2022**, *122*, 11759−11777.

(11) van Rossum, S. A.; Tena-Solsona, M.; van Esch, J. H.; Eelkema, R.; Boekhoven, J. Dissipative out-of-equilibrium assembly of man-made supramolecular materials. *Chem. Soc. Rev.* **2017**, *46*, 5519−5535.

(12) Tena-Solsona, M.; Boekhoven, J. Dissipative self-assembly of peptides. *Isr. J. Chem.* **2019**, *59*, 898−905.

(13) Yu, S.; Xian, S.; Ye, Z.; Pramudya, I.; Webber, M. J. Glucose-fueled peptide assembly: glucagon delivery via enzymatic actuation. *J. Am. Chem. Soc.* **2021**, *143*, 12578−12589.

(14) Klajn, R.; Wesson, P. J.; Bishop, K. J.; Grzybowski, B. A. Writing self-erasing images using metastable nanoparticle "inks". *Angew. Chem., Int. Ed.* **2009**, *48*, 7035−7039.

(15) de Jong, J. J.; Hania, P. R.; Pugžlys, A.; Lucas, L. N.; de Loos, M.; Kellogg, R. M.; Feringa, B. L.; Duppen, K.; van Esch, J. H. Light-Driven Dynamic Pattern Formation. *Angew. Chem.* **2005**, *117*, 2425−2428.

(16) Rakotondradany, F.; Whitehead, M.; Lebuis, A. M.; Sleiman, H. F. Photoresponsive Supramolecular Systems: Self-Assembly of Azodibenzoic Acid Linear Tapes and Cyclic Tetramers. *Chem.—Eur. J.* **2003**, *9*, 4771−4780.

(17) Selmani, S.; Schwartz, E.; Mulvey, J. T.; Wei, H.; Grosvirt-Dramen, A.; Gibson, W.; Hochbaum, A. I.; Patterson, J. P.; Ragan, R.; Guan, Z. Electrically Fueled Active Supramolecular Materials. *J. Am. Chem. Soc.* **2022**, *144*, 7844−7851.

(18) Angulo-Pachón, C. A.; Miravet, J. F. Sucrose-fueled, energy dissipative, transient formation of molecular hydrogels mediated by yeast activity. *Chem. Commun.* **2016**, *52*, 5398−5401.

(19) Jo, H.; Sim, S. Programmable Living Materials Constructed with the Dynamic Covalent Interface between Synthetic Polymers and Engineered B. subtilis. *ACS Appl. Mater. Interfaces* **2022**, *14*, 20729−20738.

(20) Otto, M. Staphylococcus epidermidis - the 'accidental' pathogen. *Nat. Rev. Microbiol.* **2009**, *7*, 555−567.

(21) Brooks, W. L.; Deng, C. C.; Sumerlin, B. S. Structure-Reactivity Relationships in Boronic Acid-Diol Complexation. *ACS Omega* **2018**, *3*, 17863−17870.

(22) Springsteen, G.; Wang, B. Alizarin Red S. as a general optical reporter for studying the binding of boronic acids with carbohydrates. *Chem. Commun.* **2001**, *17*, 1608−1609.

(23) Lindgren, J.; Thomas, V. C.; Olson, M.; Chaudhari, S.; Nuxoll, A. S.; Schaeffer, C.; Lindgren, K.; Jones, J.; Zimmerman, M. C.; Dunman, P.; Bayles, K. W.; Fey, P. D. Arginine deiminase in Staphylococcus epidermidis functions to augment biofilm maturation through pH homeostasis. *J. Bacteriol.* **2014**, *196*, 2277−2289.

(24) Marco-Dufort, B.; Iten, R.; Tibbitt, M. W. Linking molecular behavior to macroscopic properties in ideal dynamic covalent networks. *J. Am. Chem. Soc.* **2020**, *142*, 15371−15385.

(25) Piest, M.; Zhang, X.; Trinidad, J.; Engbersen, J. F. pH-responsive, dynamically restructuring hydrogels formed by reversible crosslinking of PVA with phenylboronic acid functionalised PPO-PEO-PPO spacers (Jeffamines). *Soft Matter* **2011**, *7*, 11111−11118.
(26) Jiang, M.; Li, Q.; Hu, S.; He, P.; Chen, Y.; Cai, D.; Wu, Y.; Chen, S. Enhanced aerobic denitrification performance with Bacillus licheniformis via secreting lipopeptide biosurfactant lichenysin. *Chem. Eng. J.* **2022**, *434*, 134686.

https://doi.org/10.1021/jacs.2c11122
J. Am. Chem. Soc. 2023, 145, 1811−1817